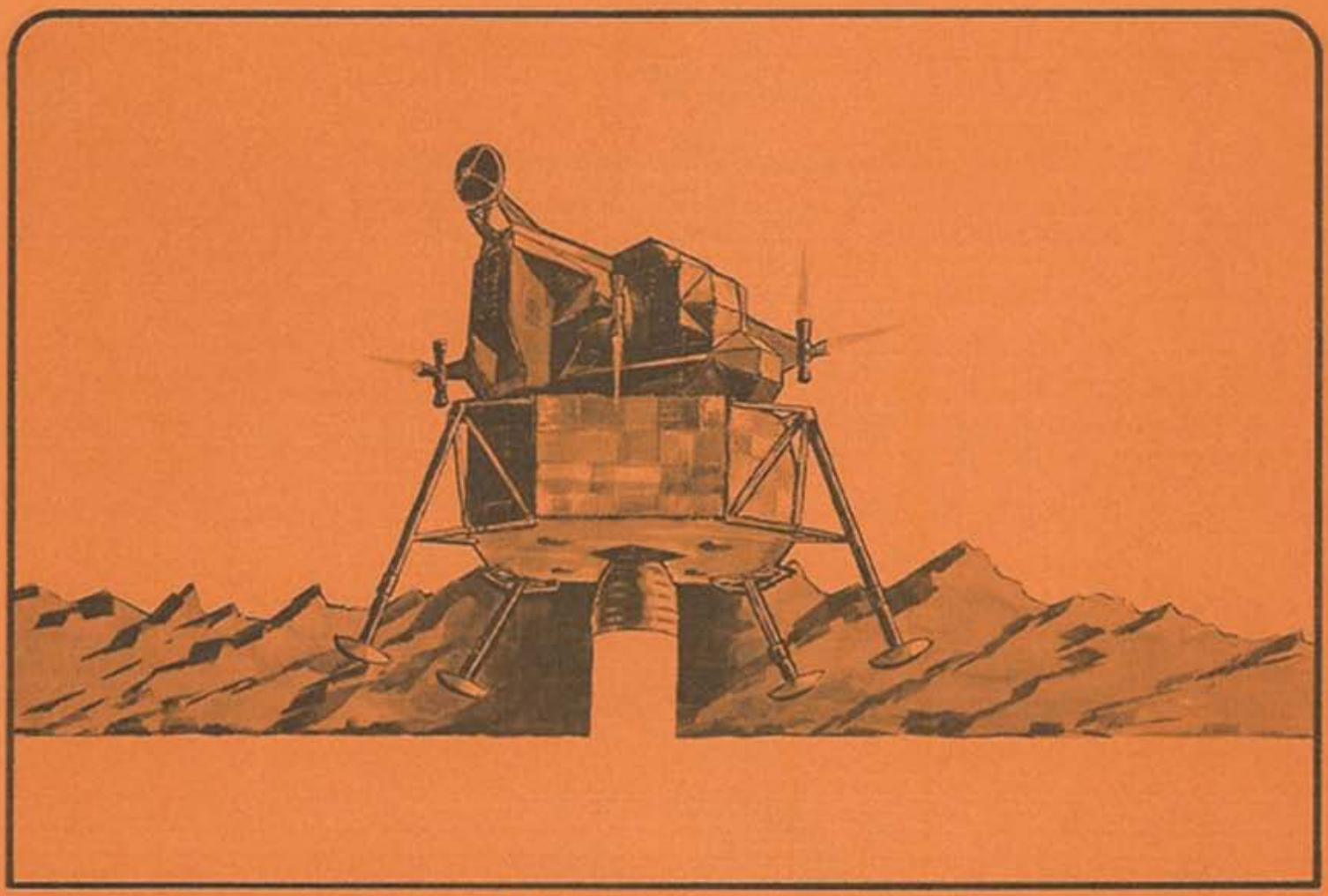

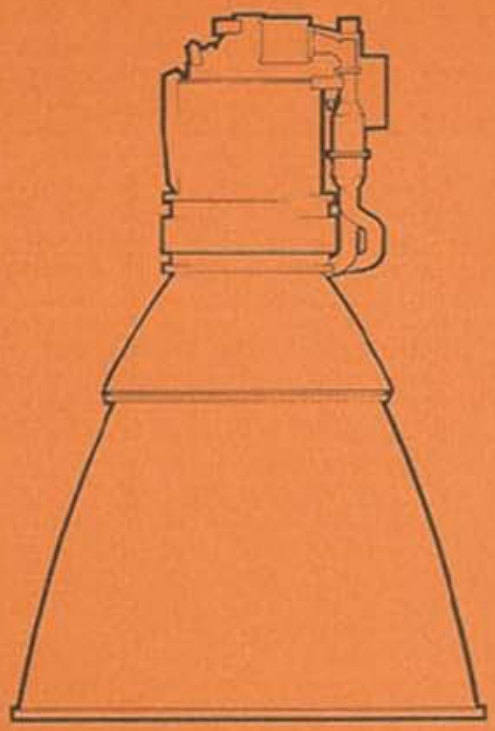

MECHANICAL DESIGN OF THE LUNAR MODULE DESCENT ENGINE

BY JACK M. CHERNE

TRW
SYSTEMS GROUP

MECHANICAL DESIGN OF THE LUNAR MODULE DESCENT ENGINE

by Jack M. Cherne

Manager, Engineering Design Department
Power Systems Division
TRW Systems
Redondo Beach, California, U.S.A.

Introduction

To land astronauts on the moon, the Lunar Module must descend from a lunar orbit to a hovering position above the surface of the moon, select a site and descend to a soft landing. TRW Systems has translated these propulsion requirements into the Lunar Module Descent Engine (LMDE).

The LMDE is a pressure-fed, bipropellant, variable thrust, gimballing, chemical rocket engine with a maximum thrust of 9850 lbs, throttleable down to approximately 1000 lbs. The throttling is obtained by means of dual, variable area, cavitating venturi flow control valves mechanically linked to a variable area injector. Ignition is hypergolic in the combustion chamber since the propellants are nitrogen tetroxide (N_2O_4) and a 50-50 mixture of hydrazine (N_2H_4) and unsymmetrical dimethylhydrazine (UDMH).

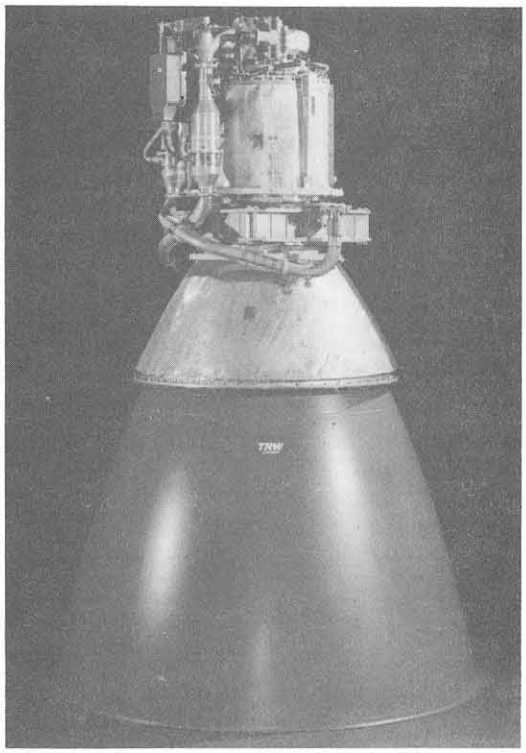

Figure 1. Lunar Module Descent Engine

The time available for developing and qualifying the LMDE for manned flight was short. To assure that unforeseen problems did not develop during the latter part of the development and qualification phase, it was important to plan an adequate component test program early in the engine's development. This program included tests of details and subassemblies to locate weaknesses in the design. Upon correction of these deficiencies, the next level of assembly was tested. Then, step by step assurance was developed that the complete engine performed as required. Details of the mechanical design of the LMDE (Figure 1) are described later in the paper. All aspects of the design, including discussion of the critical environments and the development problems anticipated, are presented along with the component tests used to find the solutions to these problems.

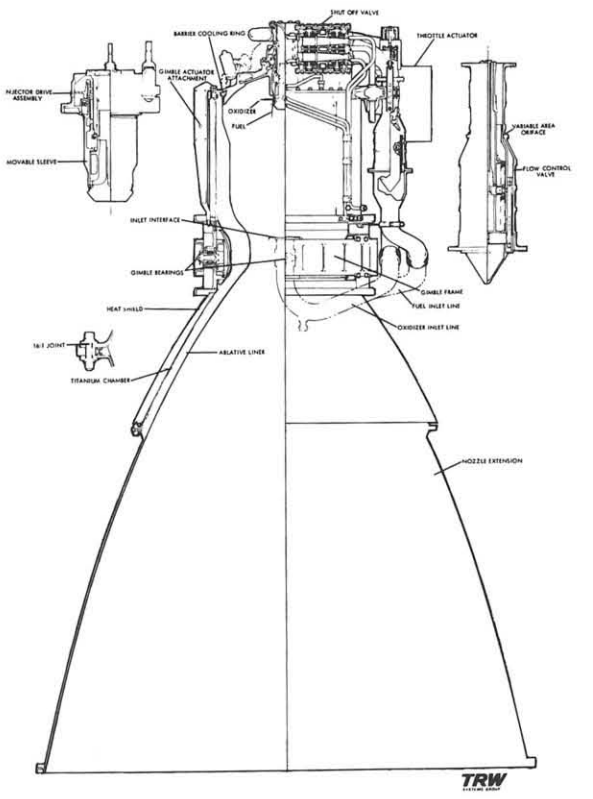

Figure 2.

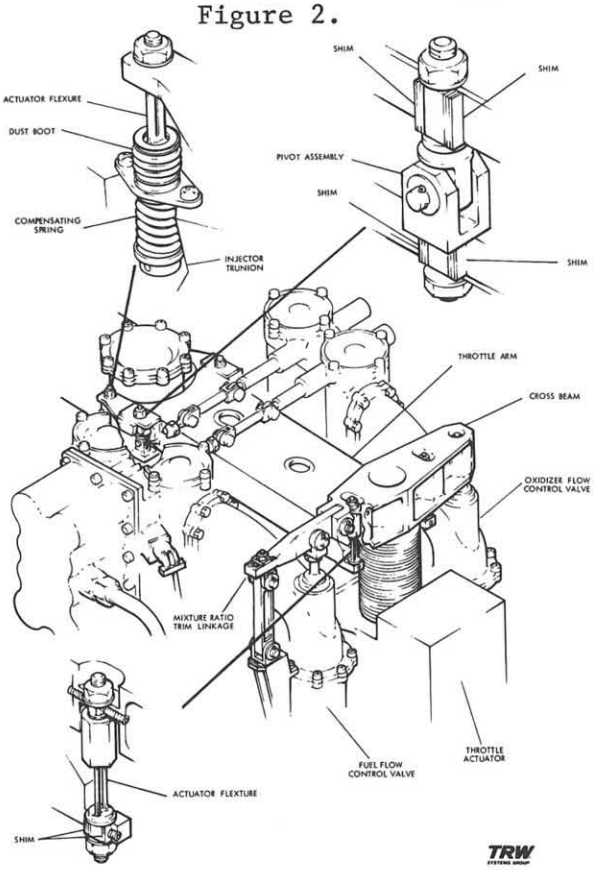

Figure 3. Thrust Control Assembly

Engine Description

The LMDE is a compact package weighing 394 lbs and having overall dimensions of 90-1/2 inches by 59 inches diameter. Interface with the Lunar Module vehicle is made at two trunnions through the gimbal frame, providing capability of gimballing 6° in both lateral directions (Figure 2). Propellants are supplied to the LMDE through two stainless steel propellant inlet lines with a simple bolted flange interface joint. The inlet lines accommodate the 6° of gimbal motion by means of a pair of flexible bellows welded in the lines at their intersection with the gimbal axes. Propellants flow from the lines through the cavitating venturi flow control valves to the quad-redundant ball shutoff valves. From the shutoff valve, the fuel enters the manifold of the head end. The major percentage of the fuel is injected axially into the combustion chamber through the annular orifice of the variable area concentric injector, while the remainder is distributed to the 36 ports of the barrier cooling ring where it is injected along the wall of the chamber. The oxidizer enters the center of the injector assembly, flows down and is directed into the combustion chamber radially through the variable area ports in a horizontal disc composed of 36 jets which impinge on and ignite with the sheet of fuel.

Thrust control is accomplished by adjusting the propellant flow rates and varying the area of the injection ports to maintain near uniform velocities. Electrical control signals from the Lunar Module are received by the electromechanical throttle actuator which converts the signal to a linear position of the actuator screw jack (Figure 3). Attached to the top of the screw jack is a cross beam. The right side of the cross beam is connected directly to the oxidizer flow control valve through a flexural element. The left side of the cross beam

is connected to the fuel flow control valve through the mixture ratio trim linkage, establishing the desired motion of the fuel flow control valve relative to the motion of the oxidizer flow control valve. This produces the required mixture ratio of the propellants. This linkage permits adjustment of the mixture ratio during acceptance tests of the engine. Also attached to the cross arm by means of two flexures is a walking beam, pivoted off the manifold assembly, which translates motion from the throttle actuator assembly to the injector assembly. Motion of the movable sleeve in the injector simultaneously changes the gap in the fuel orifice and the size of the ports in the oxidizer outlets.

The manifold assembly which provides the mounting points for the throttle mechanism is the distribution network for the propellants and the end closure of the combustion chamber. A welded titanium shell which bolts to the manifold forms the structural element of the combustion chamber and the throat of the engine. The phenolic-fiberglass ablative liner provides the thermal barrier between the burning propellants and the structural case. Attachments are provided in the throat area for the gimbal assembly. The chamber and ablative liner extend to the 16:1 area ratio point where a flanged joint provides for attachment of the nozzle extension.

The nozzle extension is a radiation-cooled, bell-shaped cone which provides for expansion of the gases from the 16:1 area ratio at the attachment to the combustion chamber to the 47.5:1 area ratio exit.

The total firing time requirement for the LM Descent Engine is 1000 seconds. This is composed of 90 seconds of acceptance testing plus 910 seconds of duty cycle. A nominal duty cycle is shown in Figure 4. Temperature of the titanium combustion chamber case does not exceed 800°F during duty cycle firing.

Thermal requirements for the Lunar Module require that the external temperature around the engine above the nozzle extension remain below 400°F during the duty cycle firing. This is accomplished by the use of a composite stainless steel and fiberglass insulating blanket around the combustion chamber.

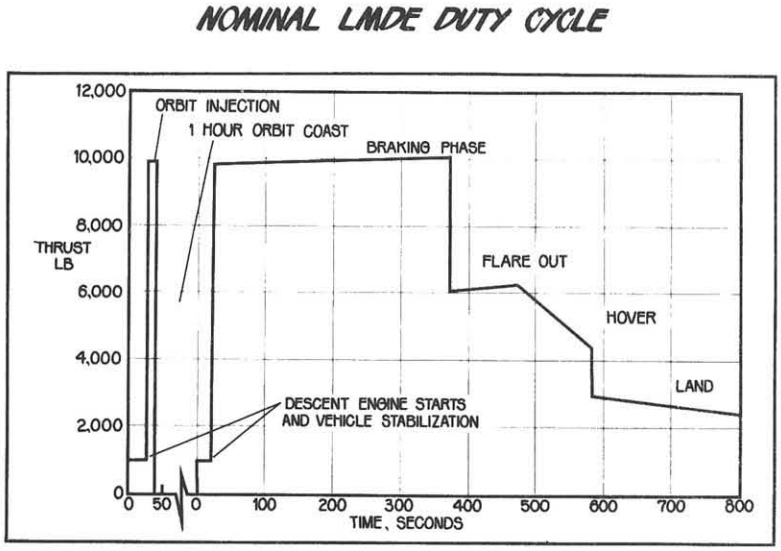

Figure 4.

Engine Gimbal

The gimbal assembly is a rectangular frame composed of four beams with a modified I section machined out of 7075-T73 aluminum alloy. The flanges of the beams are tapered in thickness and planform for minimum weight. A trunnion attaches to the center of each beam through a spherical Fabroid bearing. One pair of trunnions mounts to the engine thrust chamber and the other pair mounts to the Lunar Module support truss (Figure 5).

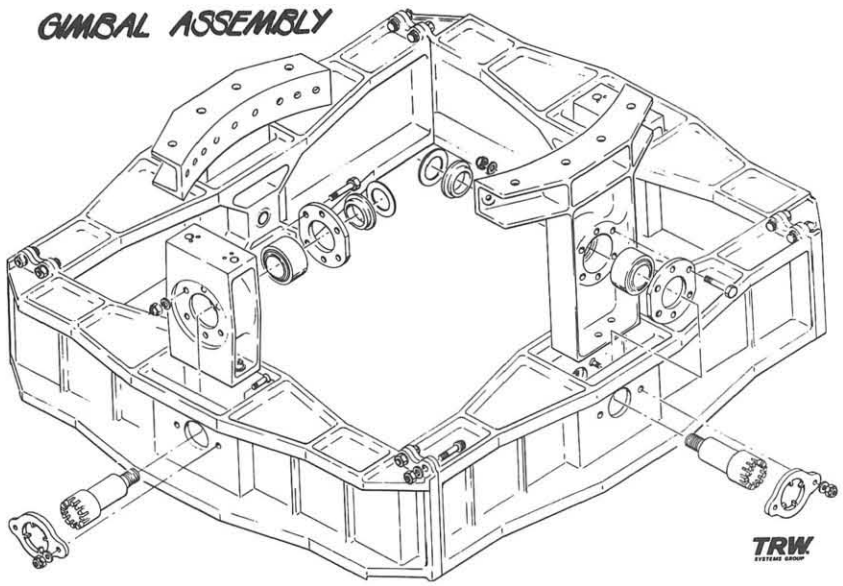

Figure 5.

Thirteen load conditions were defined as applicable to the gimbal frame. These included pre-launch shock, launch and boost vibration, engine start, lunar descent and lunar landing. Preliminary structural analysis indicated that seven of these were critical. Thermal analyses provided a maximum temperature in the gimbal beams of 200°F at the end of the mission. Ultimate static and sinusoidal load factors of 1.5 were used. An ultimate load factor of 2.25 was applied to random vibration environments.

Prior to the tests of the complete engine in the gimbal frame for dynamic environment, several component tests were conducted to ensure that these components would survive their load and life requirements.

After the selection of the configuration of the gimbal, two test programs were initiated and completed successfully before the total system tests were started. These were a static structural test to destruction of one side of the gimbal frame and a series of life cycle tests on individual gimbal bearings for shock, cyclic rotation and vibration.

Since the aluminum gimbal frame was designed for minimum weight, the static test of the single side beam was used to substantiate the stress analysis of the tapered flange members. Subjecting an individual Fabroid bearing to the cyclic rotations experienced during gimballing of the engine

during lunar descent, in addition to the shock and vibration environment of launch and boost and engine firing, revealed the need to make some changes to the bearing design. Those changes were accomplished before tests of a full gimbal frame was scheduled to start.

When a complete gimbal assembly was available for further testing, an engine assembly still could not be used; therefore, it was planned to use an engine mass simulator. This unit simulated the mass properties in the Y and Z axes but not in the X axis (the centerline of the engine thrust).

The gimbal was first subjected to the environments of salt fog, sand and dust and a limit load test to several of the critical loads. A breakaway torque test on the bearings while subjected to a thrust load of 10,500 lbs was used as one criteria for acceptance of the gimbal after each test. Alignment of the thrust axis was another criteria.

Shock tests of the gimbal with the engine mass simulator were conducted about all three axes. A shock impulse of 15 g peak with a 6 millisecond rise time was applied three times along each axis. During the shock test the gimbal was rigidly attached to the shock test equipment. No unexpected responses were noted.

Vibration tests of the gimbal frame were next performed. For this test the gimbal trunnions were mounted to a structure which simulated the influence coefficients of the Lunar Module support structure. See Figures 6 and 7. During the first sinusoidal vibration sweep along the Y axis an unexpected torsional mode was observed at 18 cps. Strain gages were installed on the gimbal frame to measure bending stresses due to the torsion and the survey repeated. As a result of the data obtained, it became apparent that it was necessary to correctly simulate the moment of inertia of the engine mass simulator about the X axis. The first simulation of I_{xx} was 34,000 lb-in^2 while the calculated engine inertia was 66,000 lb-in^2. The change in inertia was made and the vibration test completed. These tests pointed out a minor structural weakness which would have delayed the qualification tests if not discovered at this time. The bolt which attached the bearing to the gimbal frame was restrained against rotation by means of two cotter pins. These pins failed in shear permitting the bolt to rotate during vibration. Retention of the bolt was changed to the heat treated, machined lock ring shown in Figure 8.

This specimen was then subjected to mechanical cycling of ± 6° for 500 cycles about each of the rotational axes while subjected to 10,500 lbs of thrust load.

Upon completion of the mechanical cycling test, a static test to ultimate loads was performed for the most critical load conditions. Then load was applied until failure for the most critical condition with thrust applied at 6° in both directions from center. Failure occurred at 39,800 lbs which is 1.92 times the ultimate load taking account for gimballed angle, thermal degradation and other structural loads. See Figure 9.

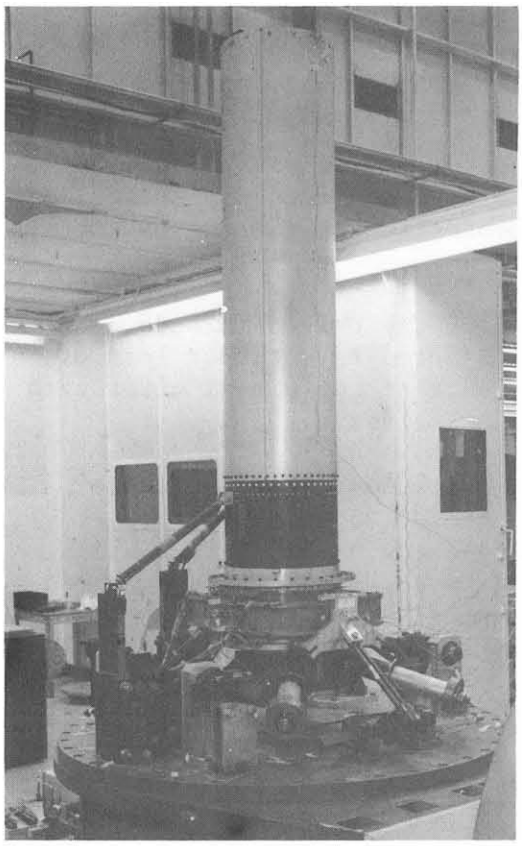

Figure 6. Engine Mass Simulator Mounted in Gimbal Frame on Vibration Test Fixture

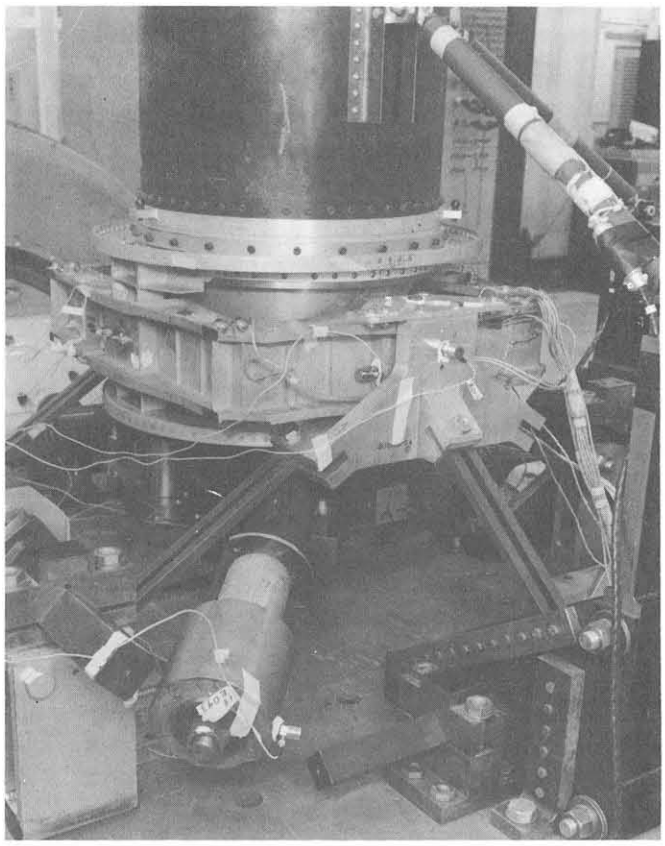

Figure 7. View of Simulation of Lunar Module Support Structure

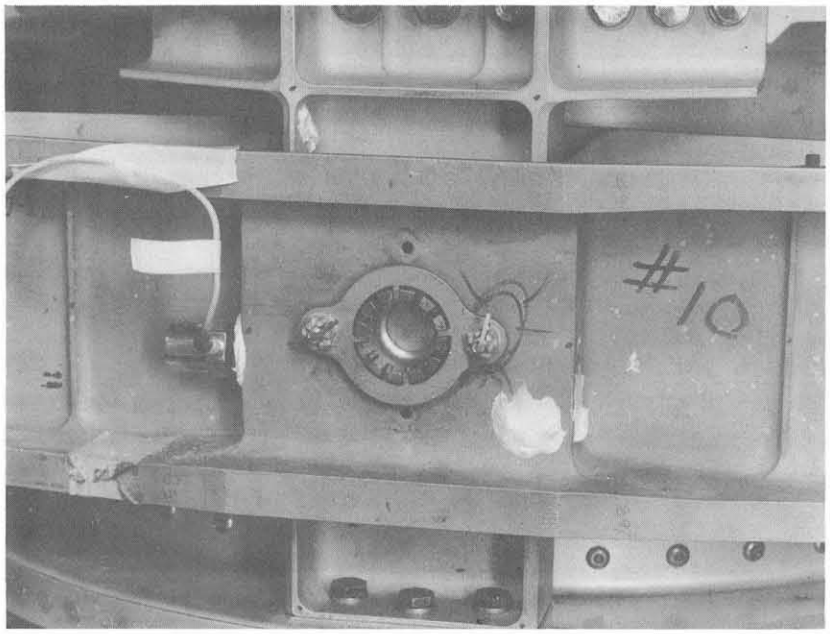

Figure 8. Redesigned Bearing Bolt Retention on Gimbal Frame

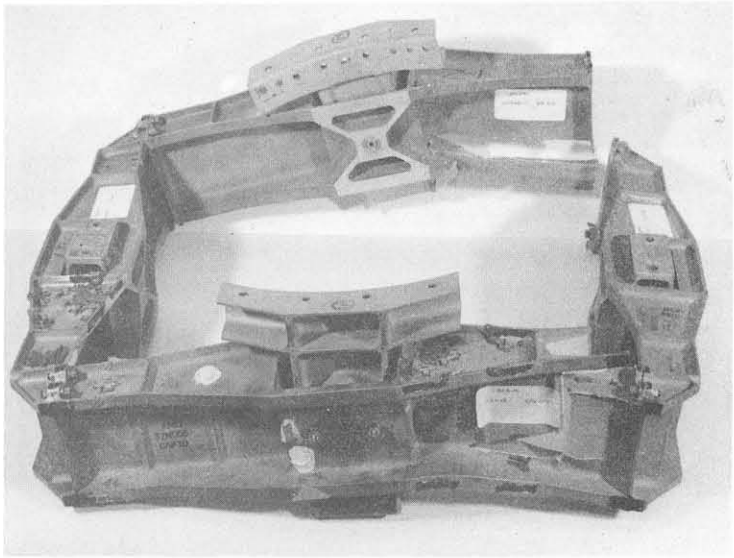

Figure 9. Gimbal Frame Static Test Specimen

Stress levels in the gimbal frame which were higher than anticipated during analysis due to the unexpected torsional mode aroused concern over the fatigue strength of the assembly. The subject test specimen was exposed to eleven times as many sinusoidal vibration cycles in the frequency range of 5 to 100 cps as is required for qualification. In addition, the exposure to random vibration was more than six times that required for qualification. Since the specimen withstood almost twice the ultimate load after experiencing all of this dynamic environment, confidence in its ability to perform during a lunar mission was established.

As a result of the knowledge gained during the early component tests and the gimbal frame tests with the engine mass simulator in October 1965, the gimbal on the design verification test of the complete engine in April 1966 and on the vibration test of the qualification engine in October 1966 performed without incident.

Combustion Chamber

The combustion chamber consists of an ablative-lined titanium alloy case to the 16:1 area ratio. Fabrication of the 6Al-4V alloy titanium case is accomplished by machining the chamber portion and the exit cone portion from forgings and welding them into one unit at the throat centerline. Thickness of the shell is a uniform 0.035 inch except at the upper end where the head end bolts on, at the weld joint and at the lower flange where the nozzle extension attaches. On either side of the throat a pair of flanges are provided integral with the case for attachment of Z-shaped aluminum rings. These rings form the structural members for attachment of the gimbal trunnions. See Figure 10.

Since the titanium chamber is one piece, the ablative liner is fabricated in two segments and installed from either end. A metal locking element positively locks both halves of the liner together as they are installed. This lock is redundant since the shape of the nozzle extension

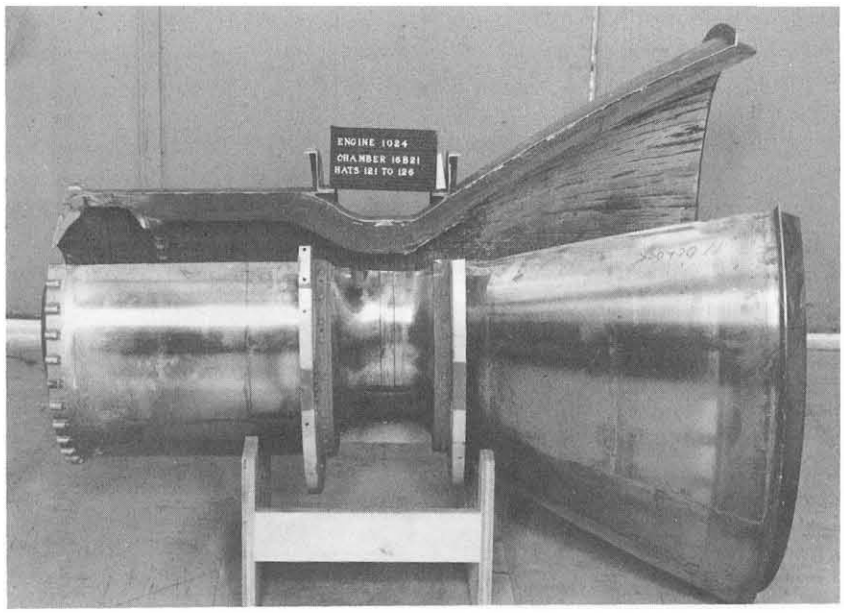

Figure 10. Combustion Chamber Assembly

is such that the ablative liner is retained in the exit cone during transportation and launch and boost. During engine firing, thrust loads force the exit cone liner against the case.

The titanium head end assembly attaches to the combustion chamber with thirty-six A-286 steel 1/4 inch bolts. This joint also permits the transfer of moments around the corner insuring a continuous pressure vessel.

In order to keep the maximum operating temperatures of the titanium case in the vicinity of 800°F, the ablative liner was designed as a composite material providing the maximum heat sink at minimum weight. The selected configuration consists of a high density, erosion-resistant silica cloth/phenolic material surrounded by a lightweight needle-felted silica mat/phenolic insulation.

Temperature of the area around the combustion chamber is maintained below 400°F with the aid of a heat shield attached to the outside of the titanium case. The heat shield consists of two layers of 0.0015 inch stainless steel foil separated by fiberglass wool.

Structurally, the ablative liner is not required to be load carrying in the pressure vessel. The maximum internal pressure is 116 psi with an ultimate load factor of 3.0. Figure 11 presents the variation of chamber pressure at full thrust and shell temperature with distance along the combustion chamber used for design analysis.

To analyze the chamber shell and head end assembly for the structural loads applied, it was necessary to utilize a TRW digital computer program developed to perform static and dynamic analysis of axisymmetric thin shells of revolution subjected to arbitrary loads. Static and dynamic response of complex multi-segment shell assemblies are calculated. Loads,

including temperature effects, of arbitrary meridional and circumferential variation, are computed - the latter by expansion in a Fourier series of harmonics. Orthotropic material properties, variable stiffness in the meridional direction, discrete circumferential stiffeners, and all physically possible boundary conditions are included.

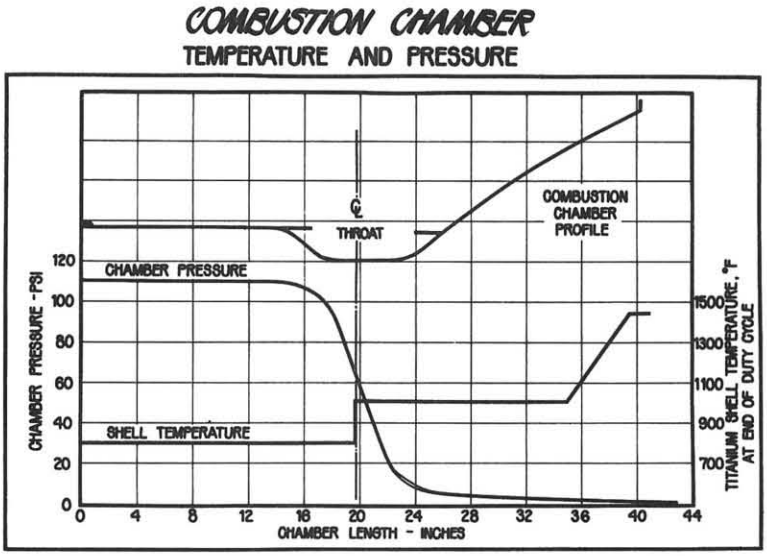

Figure 11.

The solution is based on Flügge's shell equations, which are reduced to four second-order partial differential equations in terms of the components of displacement and the meridional moment.

Substantiation of the structural integrity of the combustion chamber and head end assembly was accomplished in several steps at various stages of the program. Early in the program a room temperature burst test of an 0.050 inch thick chamber was used to check on basic material properties of the fabricated unit. This did not develop any knowledge of the complex stress distribution of the joint between the cylindrical case and the head end assembly since a heavy weight closure on the chamber was used. After the final selection of the ablative liner configuration was made and sufficient test data was accumulated to be sure of the temperature distribution in the titanium shell, it was decided that an appreciable amount of weight could be saved by reducing the case to 0.035 inch thick.

Final proof of the system was obtained by means of an elevated temperature burst test of a chamber and head end assembly, which were sealed at the throat and the interior volume of the unit reduced by filling with a metal plug. The exterior of the case was heated to 800°F with quartz lamps while pressure was applied to the interior of the assembly with argon gas. The chamber withstood 427 psig, at which time strain gages indicated that failure of the wall was imminent. The design requirement of 378 psig (three times maximum chamber pressure of 116 psig) was substantially exceeded.

Nozzle Extension

The radiation cooled nozzle extension is attached to the combustion chamber case at the area ratio of 16:1 and extends to an exit area ratio of 47.5:1. Columbium alloy C-103 was selected as the material for the nozzle extension because of its high temperature structural properties. An aluminide coating provides oxidation resistance and high emissivity.

In addition to being able to survive the aerodynamic loads of firing and the vibration environment of launch and boost, a major design criteria for the nozzle extension is that it be capable of collapsing without upsetting the Lunar Module should it strike a protrusion on the surface of the moon during landing.

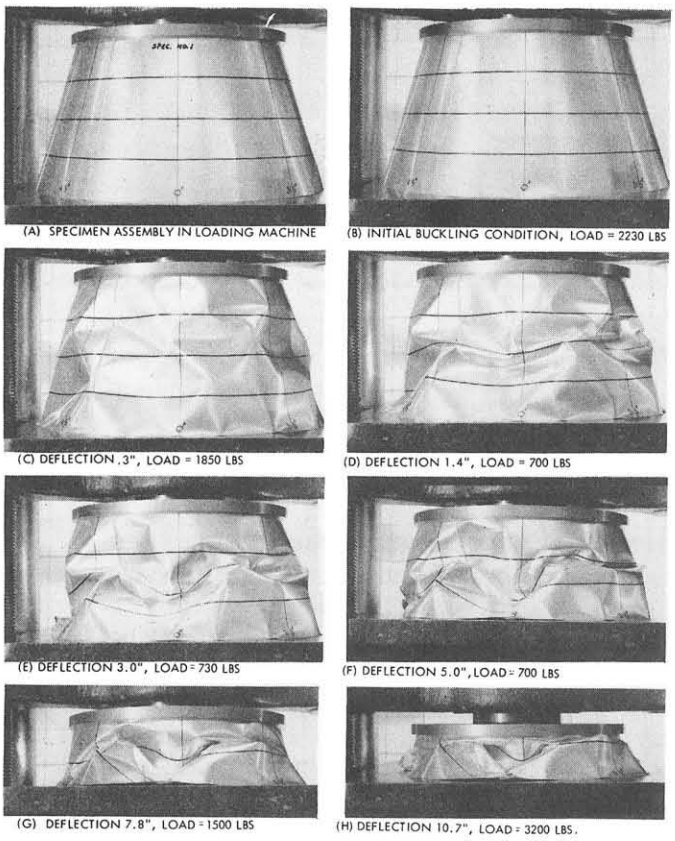

Figure 12. Aluminum Nozzle Extension Crushing Test Specimen

The program of designing a nozzle extension which would collapse 28 inches at an impact velocity of 10 ft/sec without absorbing an excessive amount of energy started in 1963 with some tests of aluminum right circular cones. Figure 12 is representative of one of the specimens. Variations of constant thickness, taper and combinations of the two were tested. The test data obtained provided assurance that the analytical methods were correct.

Having confirmed the method of analysis, a nozzle extension was designed with Haynes 25 material as a choice since the temperatures were predicted to be well below the 2400°F melting point of that material. Subsequent changes to the Lunar Module reduced the radiation cooling of the nozzle extension and the corresponding temperature profile prediction exceeded 2400°F. As a result Columbium alloy C-103 was used on the new nozzle extension since that material, when coated with the aluminide coating, can withstand temperatures up to 2700°F. The configuration consists of sheet welded in segments, stepped down in thickness towards the exit plane. At the attachment plane to the combustion chamber, the thickness is 0.060 inch in order to have a stiff surface for the seal between components. Three and one-half inches below that is a nine-inch segment 0.030 inch thick. The next 13-inch segment is 0.020 inch thick and the last 15 inches is 0.010 inch thick. At the exit plane a titanium I-shaped ring is attached

in order to provide stiffness during handling and launch and boost vibration. Figure 13 shows the temperatures measured during a high altitude test firing.

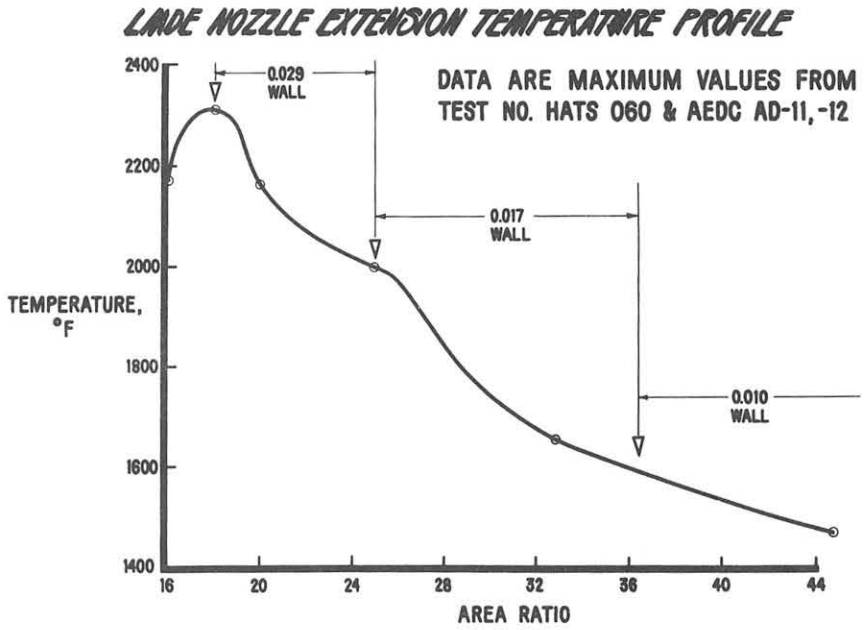

Figure 13.

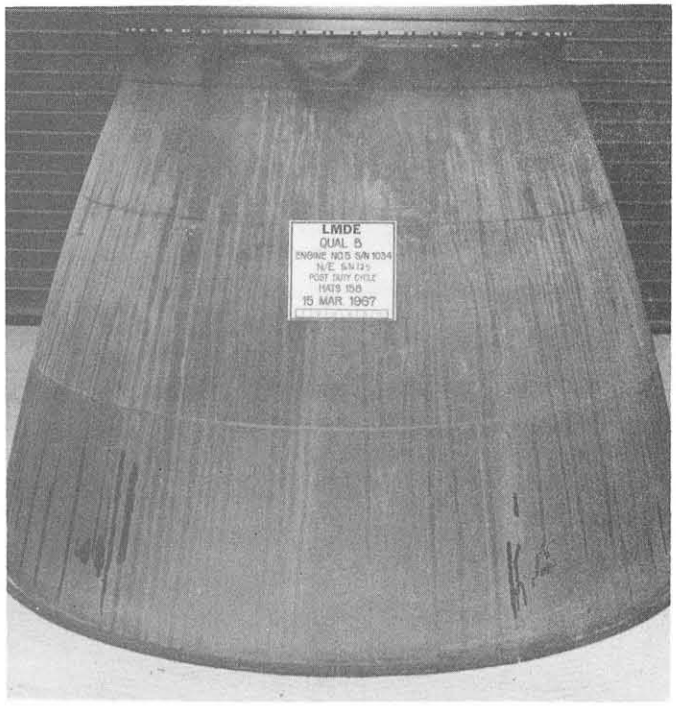

Figure 14. LMDE Nozzle Extension

Thicknesses shown in this chart are actual measurements of that specimen. One of the nozzle extensions which was used on the qualification test engines is shown in Figure 14 after the test was completed.

Proof that the nozzle extension would collapse as required without imparting forces large enough to upset the lunar vehicle during a 10 ft per sec descent to the lunar surface was undertaken with the aid of the test setup shown in Figure 15.

The columbium alloy nozzle extension was attached to a servo controlled hydraulic cylinder which provided energy necessary to collapse the nozzle extension exit flange against the lower platform which was instrumented for measuring load. Surrounding the test specimen was a bank of quartz lamps which heated up the columbium to the temperature simulating the condition at lunar touchdown. The temperature gradient controlled during this test was 2100°F at the

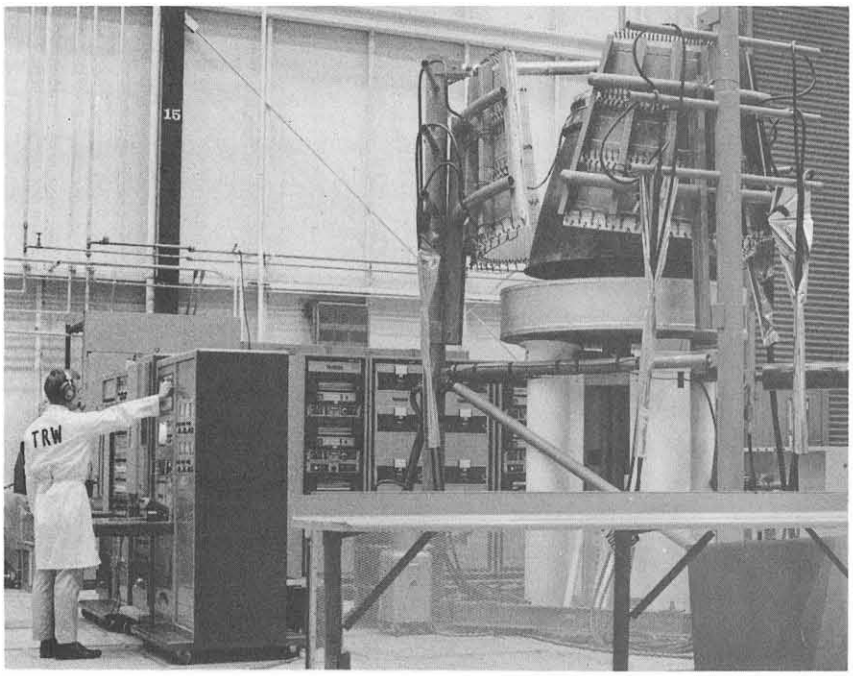

Figure 15. Nozzle Extension in Crushing Test Fixture

16:1 joint to 1250°F at the exit plane. The 10 ft per sec impact velocity was accomplished by compressing the nozzle extension 28 inches in less than 1/2 second after several inches of free motion. Resultant loads and energies recorded are shown in Figure 16.

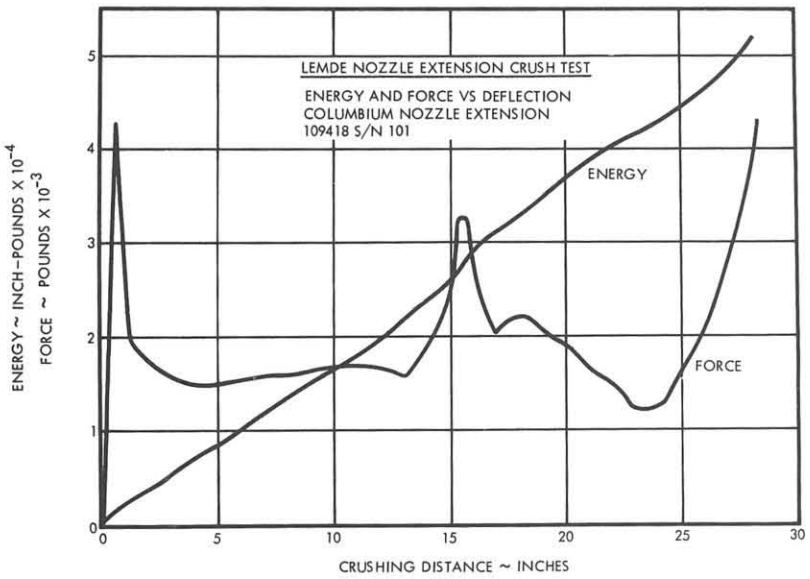

Figure 16.

Figure 17 shows the test specimen after the test. The tests performed early in the program gave assurance that the analytical methods were correct, therefore the risk taken by leaving the qualification crushing test till late in the program was small.

Figure 17. Columbium Nozzle Extension
After Crushing Test

Throttle Control Linkage

We have reviewed the structural design of the larger components of the LMDE. Now, we shall look at some of the small details which are of major importance in the function of this engine. The linkage between the throttle actuator, the flow control valves and the variable area injector drive mechanism requires high precision. The ratio between the motion of the flow control valves and the injector is 5:1. Total motion of the injector sleeve is 0.15 inch. A ten per cent increment in throttle setting is therefore a motion of only 0.003 inch. In order to maintain the position relationship between the injector sleeve and the flow control valves, looseness in the pivot bearings of the linkage had to be virtually eliminated. Another constraint on the design was that the joints of the mechanism be capable of motion in a complete vacuum.

Where possible, moving elements are connected by flexures. See Figure 3. Photographs of these flexures are shown in Figure 18. Tension and compression loads are transmitted through these flexures while they permit relative rotation of the connected members. In order to insure against a structural failure of these critical components, they were designed with redundant load paths. Either side of the flexure is capable of full load and life should one side fail.

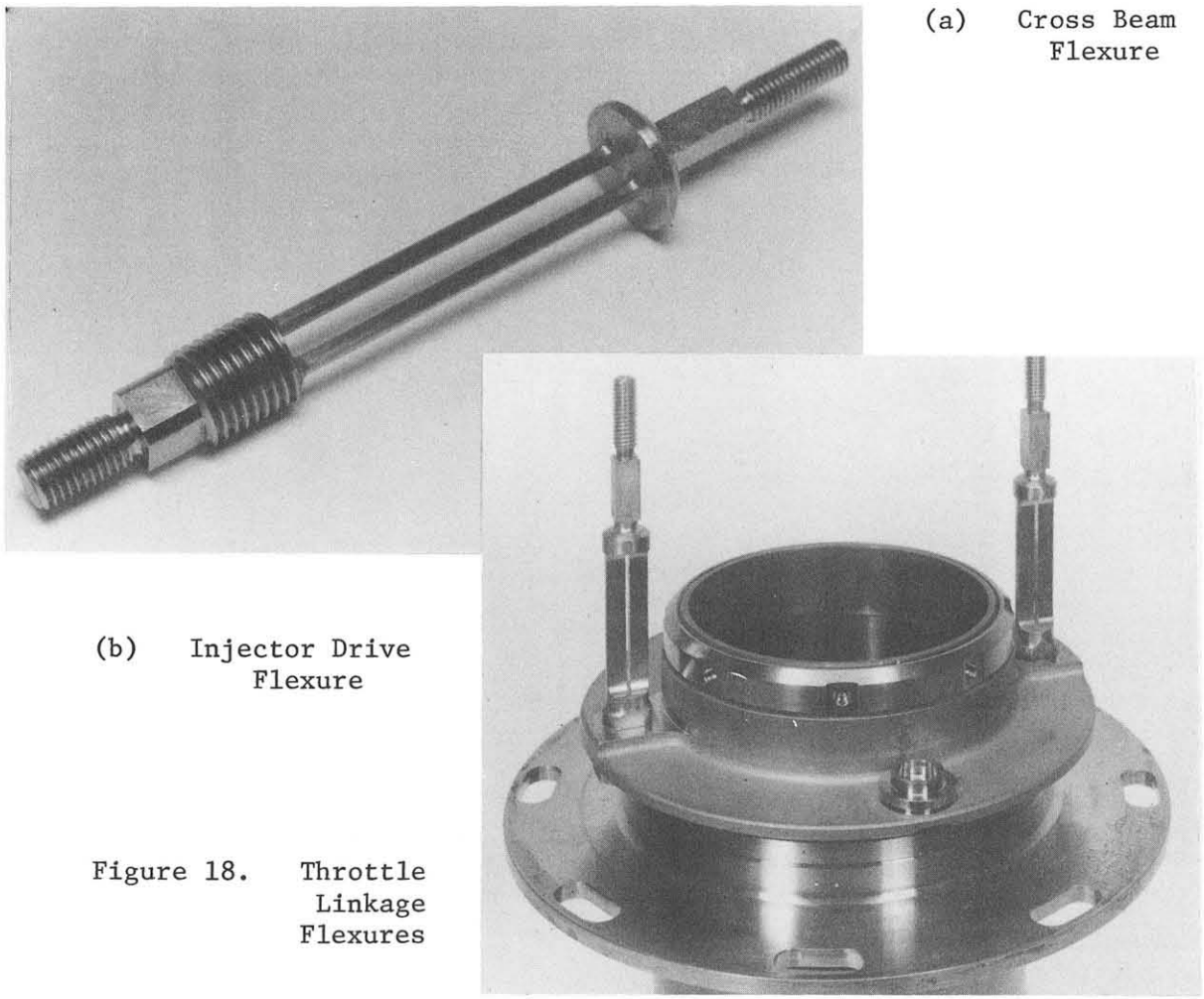

(a) Cross Beam Flexure

(b) Injector Drive Flexure

Figure 18. Throttle Linkage Flexures

In those places where a flexural element was not practical, pivot bearings were used. The first concept was to use a non-metallic bearing fabricated of fiberglass and phenolic. Initial tests showed that the wear rate of the bearing and the compliance of the material exceeded the requirements. An all metal configuration was selected. The extremely simple design consists of a steel bushing with a steel pin - both coated with molybdenum disulfide in an inorganic binder. This configuration also provides redundancy. The primary motion occurs between the pin and the inner diameter of the bushing. Should this not function, the bushing would rotate in the bore of the link of the mechanism. To substantiate the reliability of the design, an assembly of the throttle linkage was subjected to a cycling test in a vacuum chamber at 8×10^{-10} Torr. Criteria for success was completion of 10,000 cycles (33 mission duty cycles) with no significant change in load.

Proof that the complete assembly met the requirements for ruggedness, rigidity and repeatability was obtained in the deflection test shown in Figure 19. In this test motions of the two flow control valve pintles,

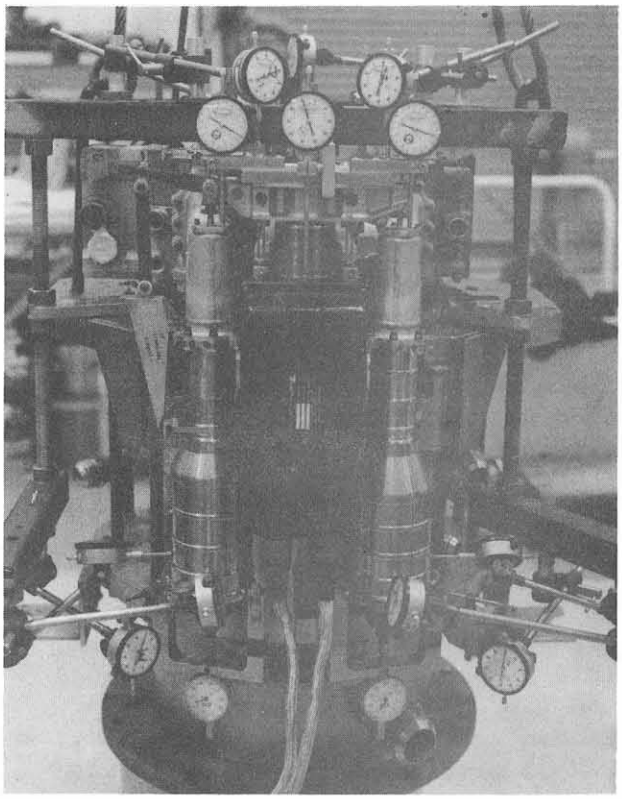

Figure 19. Deflection Test of Throttle Linkage

throttle actuator and the injector sleeve were observed and recorded under the influence of various fluid pressures and chamber pressures.

Bellows Assemblies

Both the flow control valves and the injector drive assembly contain a moving element used to control propellant flow rates while containing the propellant under pressure. Bellows are used as dynamic seals, permitting direct external actuation of internal metering surfaces. The configuration selected to accomplish this was a thin wall (0.006 to 0.010 inch) stainless steel welded bellows. Figure 20 shows the location of the bellows in the flow control valve. A similar application of bellows is used in the injector drive. In 1963 a test program to verify the strength and life of these bellows was instituted. Ten thousand cycles (33 mission duty cycles) was selected as a minimum life requirement. The original configuration did not survive the tests. Fatigue cracks occurred in the single ply convolution at the weld joints. The final configuration (Figure 21) a two-ply design with 0.004 inch convolutions successfully passed all of the tests which consisted

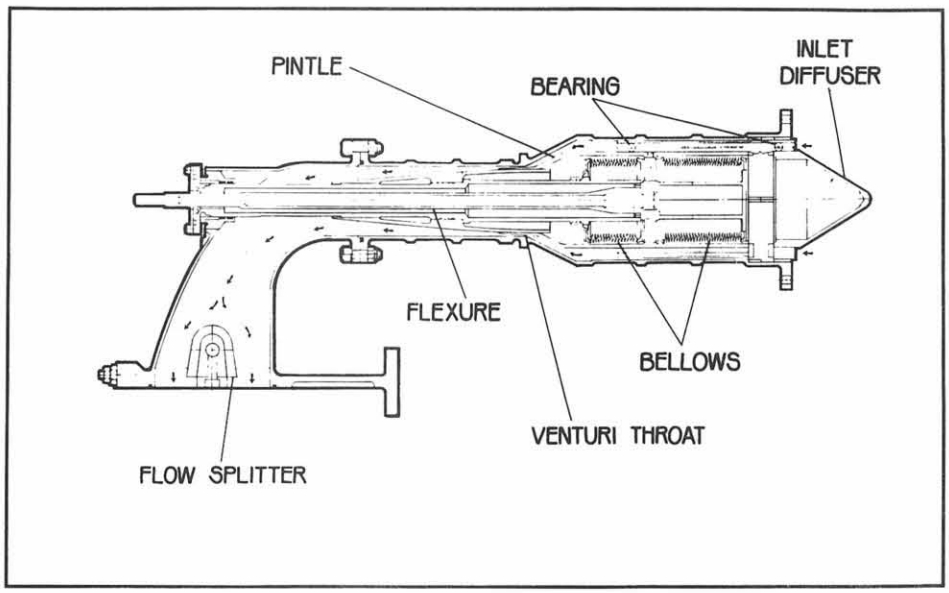

Figure 20. LMDE Flow Control Valve

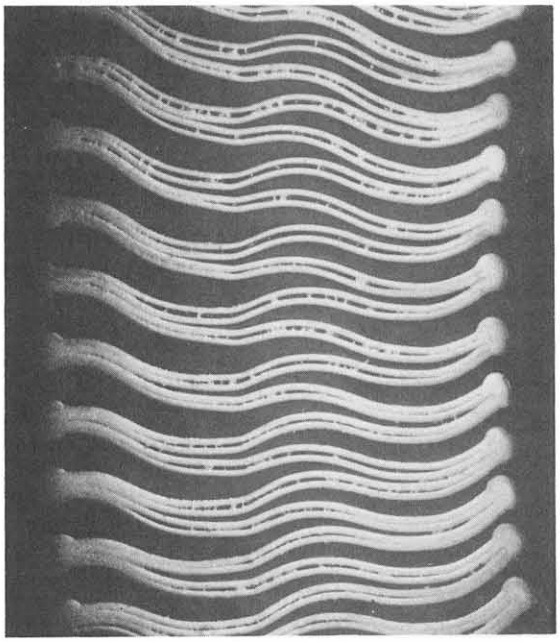

Figure 21. Section of Two-Ply Bellows

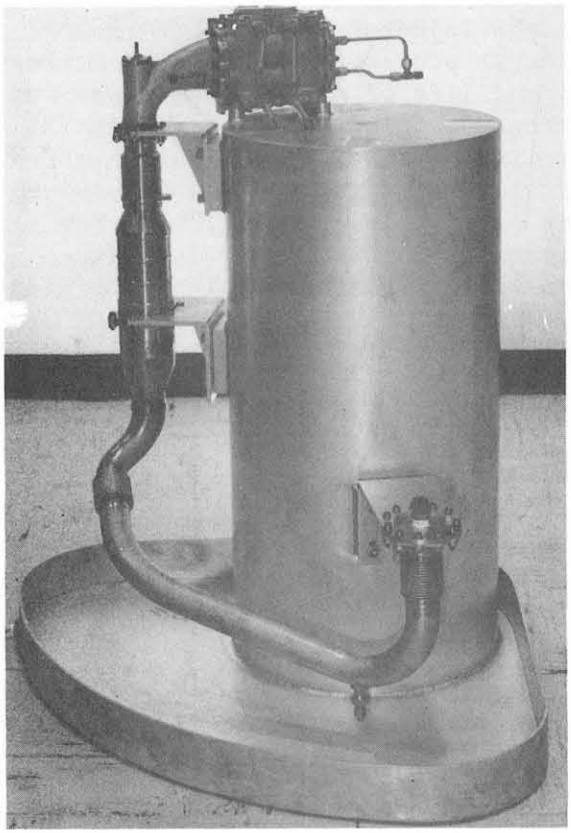

Figure 22. Component Test of Inlet Lines, Flow Control Valve and Shutoff Valve

of cycles of surge pressure, and extension and compression cycles under static pressure, followed by burst tests in excess of ten times the design pressure.

Here again, early testing of a component revealed a design deficiency which was corrected without affecting the engine development schedule. The final configuration (two-ply bellows) had an additional advantage of having a lower spring rate than the single ply bellows originally proposed.

Testing of the bellows continued when they were combined into assemblies. A component design verification test of the flow control valve included long term exposure to propellants, shock and vibration tests representing launch and boost and engine firing, and 33 mission duty cycles of pressurization and actuation. Upon completion of these exposures, the components were required to pass their acceptance criteria. Figure 22 shows the arrangement for testing the flow control valve, shutoff valve and inlet line as a subassembly.

Engine Tests

As the next step in the test program, an assembly of the head end - composed of injector manifold, injector drive, ducting, shutoff valves, flow control valves, throttle actuator, and throttle linkage - was subjected to the complete qualification level of vibration environment (Figure 23). In order to establish the margin of strength built into the head end assembly, upon completion of acceptance tests following the qualification tests, it was tested to 125% of the qual levels, then again to 150% in an attempt to find out when failure would occur. Finally failure did occur at 175% of

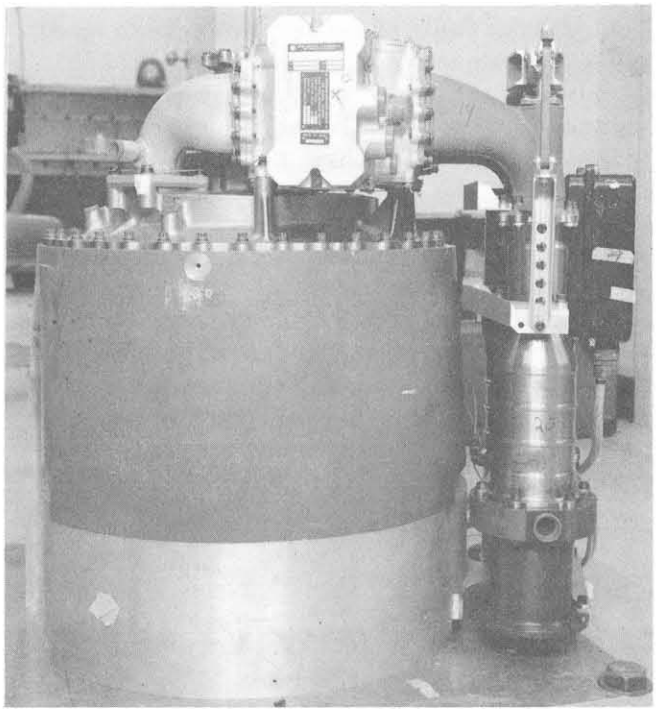

Figure 23. Vibration Test of Head End Assembly

Figure 24. LMDE Installed in High Altitude Test Stand

qualification vibration tests of the complete engine.

At this point, only the combustion chamber and nozzle extension had not been subjected to the launch and boost vibration environment. They had however received many thousands of seconds of reactive firing during the development tests of the engine in the TRW Sea Level Vertical Engine Test Stands (VETS) and High Altitude Test Stand (HATS). As a last measure before the start of the qualification series of tests, a development engine was vibration tested to the qualification environment and then successfully fired in HATS for a full mission duty cycle. The engine shown in Figure 24 installed in the HATS facility is awaiting final checkout prior to mission duty cycle firing. The support structure to which the engine is attached measures thrust and six components of thrust to determine thrust alignment.

Analysis and Test for Dynamic Loads

A linear spring-mass analogy for the LM Descent Engine was developed as a design tool to compute the dynamic loads on the engine structure. Initially, this analysis consisted of a single mass, five degree-of-freedom system. Two component masses were added to the initial analysis, increasing the number of degrees of freedom to eleven. Hand computation of the dynamic loads became very time consuming so the response equations were programed for the digital computer.

The first vibration test of the gimbal, described earlier, indicated that a strong engine torsional mode existed (engine rotation about the thrust axis). The corresponding rotational coordinate, θ_x, had been left

out of the first two analyses on the assumption that the torsional mode would not be strongly excited. Based on this experience, a third and final spring-mass model was developed. The primary purpose of this analysis was to include the torsional coordinate. In addition, the gimbal was represented as two support masses with a system of springs connecting them to the main engine mass. Each side of the gimbal is connected to the Lunar Module with a four-member truss. Modeling the gimbal in the above manner facilitated representation of the support trusses as a system of springs.

The final model is basically a three mass, twelve degree-of-freedom system (Figure 25). The motion of the main engine mass is described by six coordinates, three displacements and three rotations, in a rectangular coordinate system with the origin at the center of the gimbal. The two gimbal/support mass motions are described by three displacement coordinates each.

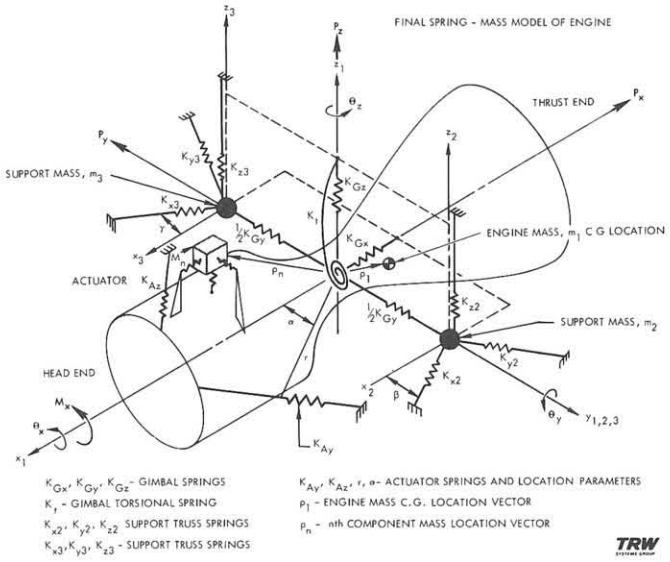

Figure 25.

Component masses can be added to the basic system to model the nozzle extension, flow control valve system, heat shield, and other engine components. Each component mass is connected to the main engine mass by three orthogonal springs and adds three degrees of freedom to the model. A thirty-six degree-of-freedom system is the most complex case run to date, although computer drum storage capabilities will allow up to 39 degrees of freedom.

The equations of motion for the model were obtained by writing the energy equations and employing the Lagrange equations. The mass and stiffness matrices from the equations of motion are put into a standard eigenvalue computer program to obtain the mode shapes and modal frequencies. This data is then input to the loads program which is based on the modal solution for sinusoidal and random base excitation. The loads program computes sinusoidal deflections and spring loads at each modal frequency by summing over the modes. It also computes the root mean square random spring loads.

Table 1 presents the qualification sinusoidal and random vibration test levels applied to the attachment interface on the gimbal frame. The configuration of the final engine vibration test specimen is shown in Figure 26. It was necessary to mount the engine upside-down in order to keep the mass of the supporting fixture low, since the mass of the fixture plus the engine approached the maximum limits of the shaker. The supporting structure is the same as used for the gimbal test shown in Figures 6 and 7.

TABLE 1

VIBRATION LEVELS FOR QUALIFICATION TEST (LAUNCH AND BOOST)

SINUSOIDAL VIBRATION

Flight Environment	Frequency	Input Level	Sweep Rate
Launch and Boost	5-16	0.2 inches d.a.	3 oct/min up and down
	16-100	2.5 g vector	

RANDOM VIBRATION

Phase	Frequency Band (cps)	Power Spectral Density	Time per Test Axis
Launch	10-23	12 db/octave rise	5 minutes
	23-80	0.025 g^2/cps	
and	80-100	12 db/octave rise	of random
	100-1000	0.06 g^2/cps	
Boost	1000-12000	12 db/octave fall	vibration
	1200-2000	0.025 g^2/cps	

Table 2 presents a comparison of the calculated and measured frequencies and loads. It is seen that the final mathematical model permits accurate estimation of the dynamic characteristics of the engine.

The analytical model has been used primarily to determine the effects of design changes. For example, following vibration of the gimbal with a mass simulated engine during design verification testing, the stiffnesses of the support trusses that mount the engine in the Lunar Module were decreased to save weight. The mathematical model was used to determine the effects of the softer mounting system on engine dynamic response. Other similar analyses include the effects of changing the gimbal actuator stiffness, effects of changing the engine c.g. location, and an evaluation of the vibration test fixture.

In addition, the dynamic loads on the gimbal nozzle extension and throttle control system have been computed for use in associated stress analyses of these components. The loads computed for the throttle control

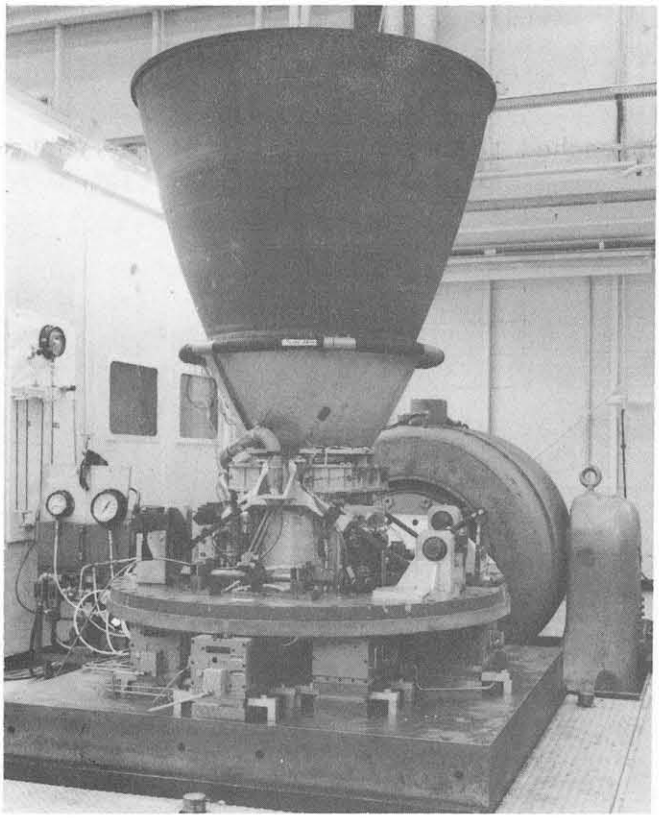

Figure 26. Vibration Test of LMDE

system, verified by the results of the engine mass simulator vibration test results, allowed simplification of the structure mounting the throttle control system on the engine.

TABLE 2

COMPARISON OF ANALYTICAL WITH TEST
DYNAMIC RESPONSE OF ENGINE

ANALYSIS MODAL FREQUENCIES (cps)	QUAL LEVEL TEST RESONANT FREQUENCIES (cps)			MAXIMUM GIMBAL LOADS		
(All Axes)	Axis			LOAD	TEST	ANALYSIS
	X	Y	Z			
11.2	11.4	11.6		M_x	28170 in-lbs	31330 in-lbs
12.6		12.7	12.7			
27.5		28.4	29.2	P_y	5580 lbs	5220 lbs
33.1	30.8	34.1	34.3	P_x	7105 lbs	7520 lbs
37.9	39.0		38.7	P_z	6723 lbs	6275 lbs

Summary

Thus at the start of the engine qualification test series, every component of the TRW Lunar Module Descent Engine had been subjected to tests - step by step - first as a unit, then in its next assembly, then as a major subassembly, and again as a complete engine. Simultaneous with all of the mechanical and structural testing described, reactive testing was being performed in the TRW facilities at San Juan Capistrano and at the USAF Arnold Engineering Development Center at Tullahoma, Tennessee, and at NASA's LM vehicle test facility at White Sands, New Mexico. Table 3 presents the detail of this test experience to 1 July 1967.

TABLE 3

LMDE REACTIVE TEST SUMMARY

	No. of New Builds	No. of Starts	Firing Duration (seconds)
Injector Tests	—	1,800	70,374
Throttling Head End Assemblies on Water Cooled Combustion Chambers	28	941	61,666
Ablative Engines			
Sea Level (ε = 2:1)	21	67	5,368
High Altitude (ε = 47.5:1)	35	242	26,549
Total Test Experience		3,050	163,957

The successful completion of qualification of the TRW LMDE demonstrates that, in order to develop light weight and reliable high performance rocket engines in a short time span, it is necessary to substantiate all of the component design concepts early in the program. A carefully designed component development test program verifies the assumptions made during design analysis and provides assurance that tests of the complete system will proceed without unexpected difficulty. The engine shown in Figure 28 being prepared for shipment to Grumman Aircraft Engineering Corporation,

designers and builders of the Lunar Module, is one of several being tested as part of the complete propulsion system and space vehicle in order to assure success for the first Lunar Module flight later this year.

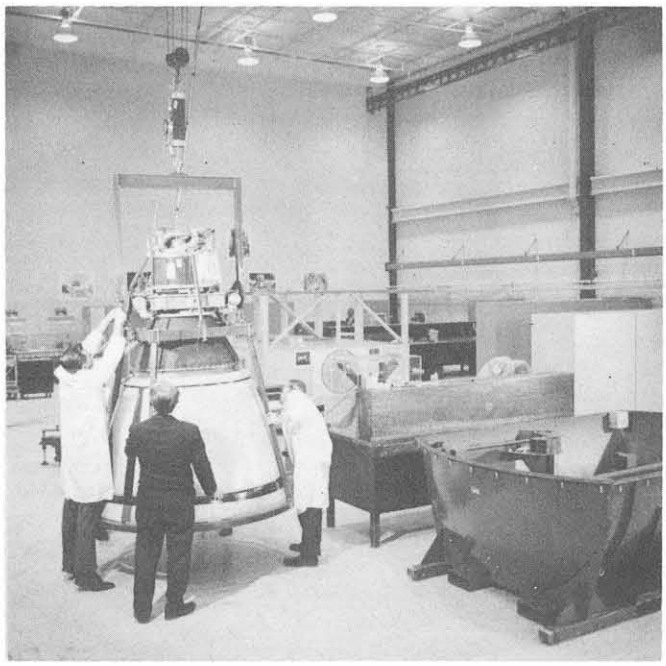

Figure 27. LMDE Being Prepared for Shipment to the Grumman Aircraft Engineering Corporation